

Long-Time Diffusion in Polymer Melts Revealed by ^1H NMR Relaxometry

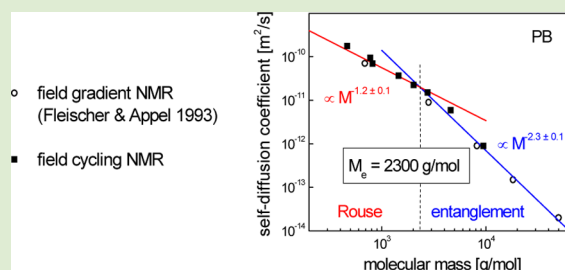
R. Meier,[†] A. Herrmann,[†] B. Kresse,[‡] A. F. Privalov,[‡] D. Kruk,[§] F. Fujara,[‡] and E. A. Rössler^{*,†}

[†]Experimentalphysik II, Universität Bayreuth, 95440 Bayreuth, Germany

[‡]Institut für Festkörperphysik, Technische Universität Darmstadt, Hochschulstr. 6, 64289 Darmstadt, Germany

[§]University of Warmia and Mazury in Olsztyn, Faculty of Mathematics and Computer Science, Sloneczna 54, PL-10710 Olsztyn, Poland

ABSTRACT: We demonstrate that field-cycling ^1H NMR relaxometry can be used as a straightforward method of determining translational diffusion coefficient $D = D(M)$ in polymer systems. The ^1H spin–lattice relaxation dispersion for polybutadiene of different molecular masses M ($446 < M/(\text{g mol}^{-1}) < 9470$) is measured at several temperatures ($233 < T/\text{K} < 408$) in a broad frequency range. The diffusion coefficient $D(T)$ is determined from the intermolecular contribution to the overall spin–lattice relaxation rate $R_1(\omega)$, which dominates in the low-frequency range and follows a universal dispersion law linear in $\sqrt{\omega}$. The extracted diffusion coefficients are in good agreement with the values obtained previously by field gradient NMR. The molecular mass dependence $D = D(M)$ exhibits two power laws: $D \propto M^{-1.3 \pm 0.1}$ and $\propto M^{-2.3 \pm 0.1}$. They show a crossover for $M = 2300$, a value that is close to the entanglement molecular mass M_e of polybutadiene. The corresponding power-law exponents are close to the prediction of the tube-reptation model.



Field-cycling (FC) ^1H NMR relaxometry has become a powerful tool for investigating dynamics of polymers.^{1,2} By varying the external magnetic field B , the frequency dependence of the spin–lattice relaxation rate $R_1(\omega) = T_1^{-1}(\omega)$ can be measured up to five decades in frequency if an earth field compensation is employed.^{3,4} By converting the relaxation dispersion into the susceptibility representation $\chi''_{\text{NMR}}(\omega) = \omega \cdot R_1(\omega)$ and then applying frequency–temperature superposition (FTS), master curves $\chi''_{\text{NMR}}(\omega\tau_s)$ are obtained; τ_s denotes the correlation time of the segmental (local) dynamics.^{2,5,6} As at low temperatures the NMR relaxation is solely determined by the segmental dynamics (other dynamical processes are too slow to act as an effective relaxation mechanism), τ_s is directly accessible. FTS is an important property of cooperative dynamics in condensed matter and has been applied for a long time, for example, in rheology of polymers. This procedure allows extending the covered frequency range and including both the polymer and the segmental dynamics into the master curve. Consequently, converting then the master curve into the time domain, the dipolar correlation function $C_{\text{DD}}(t)$ is obtained for a time range encompassing 10 decades. Characteristic power-law regimes of the correlation function can be identified and compared with the prediction of polymer theories, for example, the Doi–Edwards tube-reptation model.⁷ Moreover, the segmental mean square displacement of the polymer can be accessed in the subdiffusive regime.^{8,9}

The proton spin–lattice relaxation rate, $R_1(\omega)$, consists of intramolecular and intermolecular parts: $R_1(\omega) = R_1^{\text{intra}}(\omega) +$

$R_1^{\text{inter}}(\omega)$.¹⁰ The intramolecular contribution stems from protons belonging to the same molecule, while the intermolecular contribution originates from dipole–dipole interactions between protons of different molecules. Thus, $R_1^{\text{intra}}(\omega)$ is solely associated with molecular rotation, whereas $R_1^{\text{inter}}(\omega)$ is predominantly mediated by translational diffusion. This enables ^1H NMR relaxometry to probe the translational motion, which has recently been demonstrated for low molecular mass liquids.^{11,12} A comparison of the ^1H NMR relaxation results in the susceptibility representation with dielectric spectroscopy data has revealed that the NMR susceptibility shows a low-frequency excess contribution (of varying amplitude) in addition to the primary or α -relaxation peak.¹³ We have confirmed that the excess contribution originates from the intermolecular relaxation contributions to the total relaxation rate $R_1(\omega)$.¹⁴ The ultimate proof has been given by isotope dilution experiments,¹⁵ that is, the excess contribution disappears when the protonated molecules are substituted by their deuterated counterpart, whose interactions with protons are much weaker. The extrapolation of the relaxation data to zero concentration limit gives $R_1^{\text{intra}}(\omega)$ and, hence, also $R_1^{\text{inter}}(\omega)$.

The translational dipolar correlation function $C_{\text{inter}}(t) = \langle Y_m^{2*}(\Omega(t))Y_m^2(\Omega(0))/r^3(t)r^3(0) \rangle$ describes fluctuations of the interspin distance r and the orientation of interspin axis with

Received: October 26, 2012

Accepted: December 13, 2012

Published: January 11, 2013

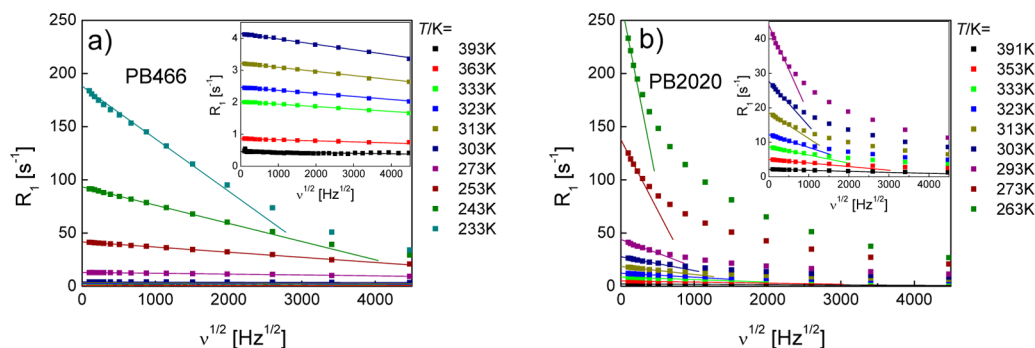


Figure 1. ¹H spin–lattice relaxation rates R_1 of polybutadiene (PB) $M = 466$ (a) and $M = 2020$ (b) plotted as a function of the square root of the Larmor frequency $\sqrt{\nu}$ in the temperature range as indicated (data from ref 3).

respect to the direction of the external magnetic field via the angle Ω encoded in spherical harmonics of rank two Y_m^2 . At long times, the correlation function follows the power law $C_{\text{inter}}(t) \propto t^{-3/2}$, which is characteristic of free diffusion.¹⁶ As a result, the spectral density (Fourier transform of the correlation function) and thus $R_1(\omega)$ depends linearly on the square root of the resonance frequency, $\sqrt{\omega}$.^{16–19} As shown for low- M liquids,¹¹ the rotational correlation time is significantly shorter than the corresponding correlation time for translational motion, as expected. Combining this dependence of the spectral density with the expression for the total ¹H spin–lattice relaxation rate,¹⁰ the low-frequency expansion (up to the first-order term and in absence of other NMR active nuclei) of the relaxation dispersion is given by^{16–19}

$$R_1(\omega) = R_1^{\text{intra}}(\omega) + R_1^{\text{inter}}(\omega) = R_1(0) - \frac{B}{D^{3/2}} \cdot \sqrt{\omega} \quad (1)$$

with

$$B = \frac{\pi}{30} \cdot (1 + 4\sqrt{2}) \cdot \left(\frac{\mu_0}{4\pi} \hbar \gamma_{\text{H}}^2 \right)^2 \cdot N$$

where γ_{H} is the proton gyromagnetic ratio and N is the spin density, that is, the number of spins per unit volume. The intramolecular contribution associated with reorientational dynamics is included in $R_1(0)$. This is allowed as the rotational contribution is frequency independent in the low-frequency range, that is, $\omega\tau_{\text{rot}} \ll 1$ (τ_{rot} denotes the rotational correlation time).

The important fact is that, besides the standard physical constants, the factor B only depends on N . It does not include any details of a diffusion model.¹⁶ Although eq 1 is well-known, its potential could have been fully exploited only lately due to commercial availability of FC spectrometers. Recently, diffusion coefficients of several liquids have been determined via eq 1 and they are in excellent agreement with those of field gradient (FG) NMR diffusometry.^{11,12}

In the present contribution, we demonstrate that the described approach can also be applied to polymer systems, and polybutadiene melts of different molecular masses M (mass average) are used as an example. There eq 1 applies for $\omega \ll 1/\tau_t$, where τ_t is the terminal relaxation time, that is, the Rouse time or the disengagement time of the tube-reptation model for nonentangled and entangled polymers, respectively (where one assumes that $\tau_t \propto D^{-1}$).

The dispersion of the spin–lattice relaxation above 10 kHz was measured by an electronic field cycling spectrometer

Spinmaster FFC 2000 manufactured by STELAR. Experiments were performed in the temperature range $233 < T/\text{K} < 408$. The relaxometer covers a ¹H frequency range from $\nu = \omega/2\pi = 10$ kHz to 20 MHz (for ¹H), while the switching time from high polarization field to relaxation field is 3 ms. Lower ¹H frequencies were reached using a home-built spectrometer in Darmstadt operating down to 400 Hz.³ The low frequencies were achieved by utilizing a three-dimensional resistive coil arrangement for compensating for the earth field and other magnetic stray fields.⁴ The relaxation rate R_1 was determined by an exponential fit of the magnetization decay curve. The results have been published previously in the susceptibility representation.³ In the present contribution we display and analyze the corresponding relaxation dispersion curves.

Figure 1a presents the spin–lattice relaxation rate R_1 plotted against the square root of the frequency $\sqrt{\nu}$ for polybutadiene (PB) with rather small molecular mass $M/(\text{g}\cdot\text{mol}^{-1}) = 466$ (PB 466). The polymer chains are still so short that essentially no polymer dynamics is discovered and the system relaxes like a low-molecular mass liquid.^{2,3} The solid lines at low frequencies indicate the limiting, linear part of the relaxation dispersion. At higher frequencies, the relaxation dispersion deviates from linearity, and the linear part shrinks with decreasing temperature (cf. inset in Figure 1a). The deviation from the linear behavior is caused by the increasing importance of higher order terms of the expansion of the translational spectral density (eq 1) and by a dispersion of the intramolecular relaxation contribution for which the extreme narrowing condition ($\omega\tau_{\text{rot}} \ll 1$) does not hold any longer.

Figure 1b shows the relaxation rates R_1 versus $\sqrt{\nu}$ for PB of $M = 2020$ which is close to the entanglement molecular mass $M_e \cong 1800$.²⁰ Again, the solid lines indicate the linear part of the relaxation dispersion observed at low frequencies. Compared to the low- M system, PB 466, the range in which $R_1(\sqrt{\nu})$ behaves linearly is rather small, but it becomes larger at high temperatures (cf. inset of Figure 1b). The pronounced difference from the data of low- M polybutadiene in Figure 1a is caused by a significantly slower as well as by a stronger relaxation dispersion due to polymer specific dynamics (cf. below).

We analyzed the relaxation dispersion for a series of polybutadienes of molecular masses $M = 466, 777, 816, 1450, 2020, 2760, 4600, 9470$ at several temperatures (data from ref 3). The procedure cannot be applied to higher M values as the linear regime in Figure 1 becomes too small or is even beyond the accessible frequency range. The relaxation data are shown as master curves in Figure 4 and discussed further below. The values of the diffusion coefficients, $D = D(T)$, are extracted

from the slope of the linear part in Figure 1 and from corresponding plots for the polybutadienes with different molecular masses using eq 1, and displayed in Figure 2. For all

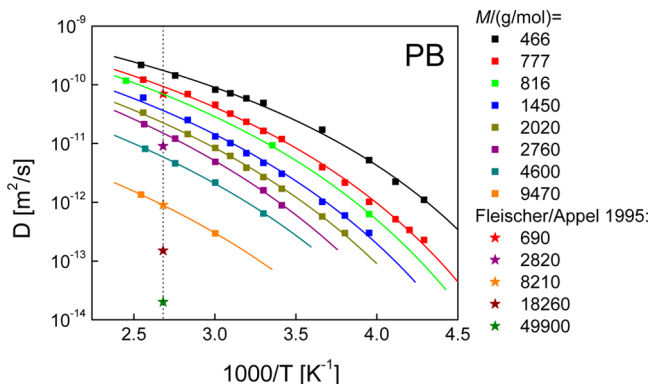


Figure 2. Diffusion coefficient $D(T)$ for polybutadiene of different molecular masses M as indicated extracted applying eq 1. Lines: interpolation by VFT equation. Stars: results from field gradient NMR at $T = 373$ K reported by Fleischer and Appel.²¹

polybutadienes, the spin density $N = 5.75 \times 10^{28} \text{ m}^{-3}$ was taken as provided by the mass density $\rho = 0.86 \text{ g/cm}^3$.²⁰ The temperature dependence of N is marginal when comparing diffusion coefficients on logarithmic scales. A super-Arrhenius temperature dependence of the diffusion coefficients is observed, and for each molecular mass $D(T)$ can be well interpolated by the Vogel–Fulcher–Tammann (VFT) equation. There is a trend that the M dependence becomes stronger at high M . Note that the temperature range in which the diffusion coefficients can be determined narrows with increasing M . For comparison, we included the results of Fleischer and Appel, which have been obtained at 373 K by applying FG NMR which is presently the standard method measuring diffusion coefficients in polymers.²¹

The M dependence of D is presented in Figure 3 and is obtained by interpolating $D(T)$ from FC NMR at $T = 373$ K (dashed line in Figure 2). The results from both FC and FG NMR nicely agree though the FC data appear to be systematically slightly higher. Two power-laws $D \propto M^{-\alpha}$ are

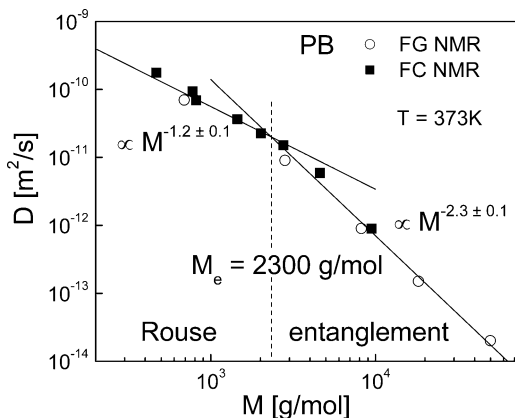


Figure 3. Dependence of the diffusion coefficient D on molecular mass M , as obtained by field cycling (FC) NMR relaxometry and by field gradient (FG) NMR;²¹ solid lines: power laws with exponents as indicated; arrow marks the crossover at a molecular mass being close to M_e .

revealed with a crossover at $M \cong 2300$, which is quite close to the entanglement molecular mass $M_e \cong 1800$.²⁰ The tube-reptation model predicts $\alpha = 1$ for the Rouse regime and $\alpha = 2$ for the entanglement regime. Fleischer and Appel have attributed all their data points to the latter regime and have reported an exponent $\alpha = 2.0$.²¹ Considering the combined results of NMR relaxometry and diffusometry, it seems that for low M the Rouse regime is already seen. By interpolating both data sets (straight lines), it has been obtained: $\alpha = 1.2 \pm 0.1$ for $M < M_e$ and $\alpha = 2.3 \pm 0.1$ for $M > M_e$. To our knowledge, this is the first time that the crossover in $D(M)$ has been found for PB. In another work, Fleischer and Appel found two regimes in the case of polydimethylsiloxane (PDMS) and polyethylene oxide (PEO).²² In the entanglement region, the exponent is similar to that found for polystyrene²³ and hydrogenated polybutadiene.²⁴ It is well-known that the tube-reptation model needs some modifications to account for effects such as constraint release or contour length fluctuations.⁷

Equation 1 implies that ^1H relaxation dispersion results obtained at different temperatures can be scaled to follow a master curve, at least at low frequencies where the expansion in eq 1 applies.¹² Thus, eq 1 can be rewritten in a master curve form:

$$R_1(\omega)/R_1(0) = 1 - \sqrt{\omega\tau_{\text{res}}} \quad (2)$$

where

$$\tau_{\text{res}} = \left(\frac{\frac{\pi}{30}(1 + 4\sqrt{2}) \left(\frac{\mu_0 \hbar \gamma^2}{4\pi} \right)^2 N}{R_1(0)D^{3/2}} \right)^2$$

In Figure 4, such master curves are displayed for a series of polybutadienes investigated in the temperature range as

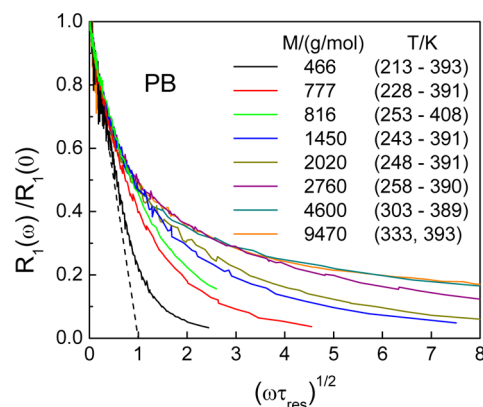


Figure 4. Master curves of PB of different M constructed from ^1H spin–lattice relaxation dispersion data obtained in the indicated temperature ranges along eq 2; dashed line: universal linear low-frequency limit.

indicated. Note that the master curves contain all relaxation data discussed in the present paper (taken from ref 3), and for a given M value, the data collapse even at high frequencies beyond the linear low-frequency regime. This is a consequence of the fact that translational-rotational coupling or more generally FTS applies in good approximation for polymer melts. The master curves for different M coincide in the linear low frequency range but systematically differ at higher reduced frequencies $(\omega\tau_{\text{res}})^{0.5}$. Whereas for PB 466 the reduced

relaxation rate $R_1(\omega)/R_1(0)$ follows the linear dependence in a wide frequency range, for the high- M polymers this regime is significantly smaller and eventually, for $M > 9470$, vanishes. The progressing bending over of $R_1 = R_1(\sqrt{\omega})$ for increasing M stems from increasing contributions of polymer specific relaxation terms reflecting Rouse and entanglement dynamics to the overall relaxation. In terms of their time-scale, they are located between the terminal relaxation and the segmental relaxation as demonstrated in our previous publications.^{2,3}

In conclusion, the present study demonstrates that the method of determining the diffusion coefficient from the low-frequency slope of the ^1H spin–lattice relaxation dispersion, as already applied to low-molecular mass liquids,^{11,12} can also be used for neat polymers. An extension to polymer solutions is not straightforward as the method probes the relative translational displacements among the proton bearing species. NMR relaxometry allows probing rotational and translational dynamics of polymer systems in a single experiment. The rotational dynamics has been discussed in our previous works, in which the temperature and molecular mass dependencies of the segmental (reorientational) contribution dominating the high-frequency behavior of the relaxation rate were analyzed in addition to the polymer specific.^{2,3,5,6} In the present work, the low-frequency features of the ^1H relaxation rate were used to complete the analysis of the polymer dynamics by extracting the diffusion coefficients and inquire into their dependence on temperature and molecular mass. Note that this evaluation is only possible by attaining the relaxation rate at extremely low frequencies. The obtained $D(M)$ data agree well with those reported by FG NMR, thus making FC NMR a further technique probing diffusion of condensed matter.

AUTHOR INFORMATION

Corresponding Author

*E-mail: ernst.roessler@uni-bayreuth.de.

Notes

The authors declare no competing financial interest.

REFERENCES

- (1) Kimmich, R.; Fatkullin, N. *Adv. Polym. Sci.* **2004**, *170*, 1–113.
- (2) Kruk, D.; Herrmann, A.; Rössler, E. A. *Prog. NMR Spectrosc.* **2012**, *63*, 33–64.
- (3) Herrmann, A.; Kresse, B.; Gmeiner, J.; Privalov, A. F.; Kruk, D.; Fujara, F.; Rössler, E. A. *Macromolecules* **2012**, *45*, 1408–1416.
- (4) Kresse, B.; Privalov, A. F.; Fujara, F. *Solid State Nucl. Magn. Reson.* **2011**, *40*, 134–137.
- (5) Kariyo, S.; Gainaru, C.; Schick, H.; Brodin, A.; Novikov, V. N.; Rössler, E. A. *Phys. Rev. Lett.* **2006**, *97*, 207803. Erratum: Herrmann, A.; Gainaru, C.; Schick, H.; Brodin, A.; Novikov, V. N.; Rössler, E. A. *Phys. Rev. Lett.* **2008**, *100*, 109901.
- (6) Kariyo, S.; Brodin, A.; Gainaru, C.; Herrmann, A.; Schick, H.; Novikov, V. N.; Rössler, E. A. *Macromolecules* **2008**, *41*, 5313–5321.
- (7) Doi, M.; Edwards, S. F. *The Theory of Polymer Dynamics*; Oxford Science Publications: Oxford, 1986.
- (8) Kehr, M.; Fatkullin, N.; Kimmich, R. *J. Chem. Phys.* **2007**, *127*, 084911.
- (9) Herrmann, A.; Kresse, B.; Wohlfahrt, M.; Bauer, I.; Privalov, A. F.; Kruk, D.; Fatkullin, N.; Fujara, F.; Rössler, E. A. *Macromolecules* **2012**, *45*, 6516–6526.
- (10) Abragam, A. *The Principles of Nuclear Magnetism*; Clarendon Press: Oxford, U.K., 1961.
- (11) Kruk, D.; Meier, R.; Rössler, E. A. *Phys. Rev. E* **2012**, *85*, 020201(R).
- (12) Meier, R.; Kruk, D.; Bourdick, A.; Schneider, E.; Rössler, E. A. *Appl. Magn. Reson.* **2012**, DOI: 10.1007/s00723-012-0410-1.
- (13) Meier, R.; Kahlau, R.; Kruk, D.; Rössler, E. A. *J. Phys. Chem. A* **2010**, *114*, 7847–7855.
- (14) Kruk, D.; Meier, R.; Rössler, E. A. *J. Phys. Chem. B* **2011**, *115*, 951–957.
- (15) Meier, R.; Kruk, D.; Gmeiner, J.; Rössler, E. A. *J. Chem. Phys.* **2012**, *136*, 034508.
- (16) Belorizky, E.; Fries, P. H. *Chem. Phys. Lett.* **1988**, *145*, 33–38.
- (17) Torrey, H. C. *Phys. Rev.* **1953**, *92*, 962–969.
- (18) Heinze, H. E.; Pfeiffer, H. Z. *Z. Phys.* **1966**, *192*, 329–339.
- (19) Harmon, J. F.; Muller, B. H. *Phys. Rev.* **1969**, *182*, 400–410.
- (20) Fetters, L. J.; Lohse, D. J.; Richter, D.; Witten, T. A.; Zirkel, A. *Macromolecules* **1994**, *27*, 4639–4647.
- (21) Fleischer, G.; Appel, M. *Macromolecules* **1995**, *28*, 7281–7283.
- (22) Fleischer, G.; Appel, M. *Macromolecules* **1993**, *26*, 5520–5525.
- (23) Antonietti, M.; Fölsch, K. J.; Sillescu, H. *Makromol. Chem.* **1987**, *188*, 2317–2324.
- (24) Lodge, T. P. *Phys. Rev. Lett.* **1999**, *83*, 3218–2321.